Large-scale *ab initio* simulations of binary transition metal clusters for storage media materials

2009 J. Phys.: Condens. Matter 21 064228

(http://iopscience.iop.org/0953-8984/21/6/064228)

J. Phys.: Condens. Matter **21** (2009) 064228 (7pp) doi:10.1088/0953-8984/21/6/064228

Large-scale *ab initio* simulations of binary transition metal clusters for storage media materials

P Entel and M E Gruner

Physics Department and Center for Nanointegration CENIDE, University of Duisburg-Essen, D-47048 Duisburg, Germany

E-mail: peter.entel@uni-due.de and markus.gruner@uni-due.de

Received 1 July 2008, in final form 22 July 2008
Published 20 January 2009
Online at stacks.iop.org/JPhysCM/21/064228

Abstract

In the quest for ultra-high-density magnetic recording, new materials in the nanometre range have attracted much interest over the last decade involving intense studies of $L1_0$ phases of contemporary or future storage media materials like FePt or CoPt nanoparticles. Based on large-scale density functional theory calculations, we provide a systematic overview of the structural and magnetic properties of various morphologies of FePt and CoPt nanoclusters with diameters up to 3 nm. In this size range, the ordered multiply twinned morphologies are energetically favoured over the nanoclusters with the desired layer type $L1_0$ and high magnetocrystalline anisotropy. Other nanoparticles of interest, like FePd, also show a preference for multiply twinned structures or exhibit, as in the case of MnPt nanoclusters, a strong tendency for antiferromagnetic ordering instead of ferromagnetic order. The compositional trends of the various nanoparticles can be traced back to differences in the partial electronic density of states of the 3d element.

(Some figures in this article are in colour only in the electronic version)

1. Introduction: transition metal nanoparticles for magnetic recording

In the search for ultra-high-density magnetic recording media, monodisperse FePt nanoparticles and ferromagnetic FePt nanocrystal superlattices have been synthesized with particle sizes tunable from 3 to 10 nanometre (nm) diameter [1]. For the larger nanoclusters, thermal annealing may transform the individual particles into the chemically ordered face centred tetragonal (fct $L1_0$) phase and the superlattice into a robust ferromagnetic (FM) nanoparticle superlattice which can support high-density magnetization reversal transitions. The $L1_0$ phase of the corresponding stoichiometric FePt bulk material exhibits a large uniaxial magnetocrystalline anisotropy constant K_u listed in table 1. Assuming that the nanoparticles can be prepared in the $L1_0$ structure with the same large magnetocrystalline anisotropy constant as the bulk material, the idea is then to use a patterned three-dimensional array of FM FePt nanoparticles as a new high-density magnetic recording media material. One of the major obstacles is the superparamagnetic limit:

$$\tau = \tau_0 \exp\left(\frac{K_u V}{k_B T}\right), \tag{1}$$

which puts a lower limit on the time τ for which the stored data are secure. Here, τ_0 is some reciprocal intrinsic frequency of the order of 10^{-9} Hz, K_u is the uniaxial anisotropy constant and V is the volume associated with the typical size of grains in current media material; values for different materials have been listed in table 1 taken from [2]. Asking for a secure storage time of ten years and using bulk quantities for the materials parameters, one may use (1) to solve for the size of the nanoparticles, which yields the diameters D_p also listed in table 1. For FePt nanoparticles, the lower limit of D_p is of the order of 3 nm. Since nanoclusters with sizes of 3 nm diameter can nowadays be simulated using density functional theory codes on massively parallel computer platforms, we have undertaken these calculations in order to check how far FePt, CoPt and a few other transition metal nanoclusters may indeed be useful as future storage media material.

Table 1. Properties of a few hard magnetic materials. Included are hcp-Co, ordered Co_3Pt and the conventional media alloy CoPtCr as well as $L1_0$ phases for future or contemporary storage media materials. For all materials, grain sizes $D_p < 10$ nm are predicted for storage times of ten years. For further data and references see [2].

Alloy system	Material	K_u (10^7 erg cm^{-3})	M_s (emu cm^{-3})	T_c (K)	H_c (kOe)	D_p (nm)
Co alloys	CoPtCr	0.20	298	—	13.7	10.4
	Co	0.45	1400	1404	6.4	8.0
	Co_3Pt	2.0	1100	—	36	4.8
$L1_0$	FePd	1.8	1100	760	33	5.0
phases	FePt	6.6–10	1140	750	116	2.8–3.0
	CoPt	4.9	800	840	123	3.6
	MnAl	1.7	560	650	69	5.1

The superparamagnetic limit is not considered a real obstacle, since in an assembly of densely packed monodisperse nanoparticles a robust ferromagnetic state is possible due to intergranular exchange and magnetic dipole interaction between the nanoparticles. Although this is a subtle point and the actual magnetic properties of assembled nanoparticles and nanocrystalline materials depend on fabrication and heat treatment, which can result in segregation effects (for example, in CoPtCr alloys, the intergrain magnetic coupling is strongly influenced by segregation of Cr towards the grain boundaries [3]), this is not a subject of the present paper.

In spite of the positive report for monodisperse FePt nanoparticles as basic ingredients for FM nanocrystal superlattices as future magnetic recording materials with densities in the terabit per square inch regime [1, 2], in many experiments only very low values for coercive field and magnetocrystalline anisotropy constant have been observed [4, 5].

Figure 1 shows coercive fields of near-stoichiometric FePt nanoclusters discussed in [4]. The data, which have been extrapolated to zero temperature from the room temperature measurement, show a sudden increase of the coercive field values for particles with diameters beyond 7 nm, although all reported values are much lower than the corresponding bulk value in table 1. The reason for low coercive fields (and hence for low magnetocrystalline anisotropy constants) may be traced back in part to the formation of multiple twins, which reduces the magnetic anisotropy to very low values.

It seems that the occurrence of multiply twinned FePt and FeCo nanoparticles with sizes below a critical diameter around a few nm is the generic case and that it is difficult to fabricate nanoclusters having the $L1_0$ structure, which is a prerequisite for a small tetragonal deformation and the appearance of large magnetocrystalline anisotropy [4, 5]. Further discussion of different morphologies of FePt and CoPt particles obtained in the fabrication process and morphology changes on substrates or when annealing to elevated temperatures can be found in [6–11]. Fabrication of oriented $L1_0$-FePt and FePd nanoparticles and exchange coupled α-Fe/$L1_0$-FePd nanocomposite isolated particles with large coercivity is discussed in [12, 13]. With respect to theory, *ab initio* calculations for $L1_0$-ordered bulk FePt have proven to be consistent with experiment regarding the temperature variation of magnetic anisotropy [14]. When performing *ab initio* calculations for FePt and other bimetallic transition metal

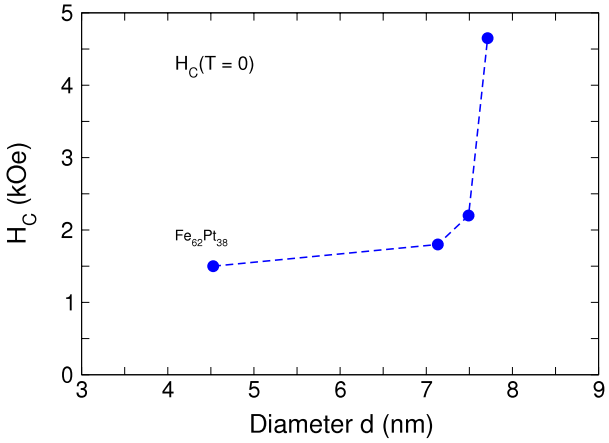

Figure 1. Coercivity of $Fe_{62}Pt_{38}$ nanoparticles as a function of the diameter; data extrapolated from room temperature measurements to zero temperature [4].

clusters, we find that the ground state morphologies differ from the $L1_0$ structure; this observation is in agreement with many experiments [15]. In the following, we present results which rely on the work in [15] which has been extended to include further candidates for future $L1_0$ phase based storage media materials.

2. Computational details of *ab initio* cluster calculations

Most results for the bimetallic transition metal clusters discussed below have been obtained from large-scale *ab initio* investigations carried out on the IBM Blue Gene/L and Blue Gene/P supercomputer systems of the John von Neumann Institute for Computing at Forschungszentrum Jülich. In the density functional theory calculations we mainly used the Vienna *ab initio* simulation package (VASP) [16] and the projector augmented wave approach [17] with a sufficiently high plane wave cutoff energy and k-space integration restricted to the Γ-point only. Since periodic boundary conditions are involved, the size of the supercell containing the nanoparticle was chosen such that the distance between atoms of the periodic images exceeded 9 Å. This was sufficient to avoid interaction of the cluster with its images. For the bimetallic clusters with a total number of 561 atoms discussed

below (265 Fe or Co and 296 Pt atoms, respectively), this required a cell size of 32 × 32 × 32 Å^3. The cutoff for the plane wave energy was set to 268 eV. In the case of FePt nanoparticles, the Fe $3d^74s^1$ and Pt $5d^96s^1$ electrons were treated as valence electrons.

All nanoclusters were allowed to perform structural relaxations, which were carried out on the Born–Oppenheimer surface using the conjugate gradient method. The structural optimization was stopped when the energy difference between two consecutive relaxations was less than 0.1 meV, leading to a convergence of forces down to the order of 10 meV Å^{-1}.

For further computational details of the *ab initio* calculations involving transition metal clusters with more than 500 atoms, we refer to [15, 18, 19].

Since for the bimetallic nanoparticles systematic *ab initio* studies are considerably more costly than for monometallic systems, as in addition to different morphologies for each cluster size, order–disorder and segregation effects have to be taken care of, a full scan of configuration space is not possible. So the investigations were limited to so-called *magic* cluster sizes

$$N = \tfrac{1}{3}\left(10n^3 + 15n^2 + 11n + 3\right) = 13,\ 55,\ 147,\ 309,\ 561,\ 923, 1425,\ \text{etc}, \quad (2)$$

where N is the total number of atoms and n is the number of closed atomic shells in the cluster. Concentrating on the magic clusters allows us to compare for each cluster size perfect cuboctahedra with fcc or fct structure, Mackay icosahedra [21] and Ino decahedra [22].

We considered disordered, ordered as well as core–shell-like arrangements of the two kinds of atoms: the latter mimics perfect segregation with all atoms on the surface or in the sub-surface shell. The compositions were fixed to $L1_0$ ordered cuboctahedra with terminating Pt layers on each side, which is energetically more favourable than Fe-terminated clusters [19]. This means that the compositions of the FePt and CoPt clusters considered, according to the cuboctahedra with perfect $L1_0$ order, must have excess Pt atoms compared to the number of Fe atoms in the cluster. For the $L1_0$ cuboctahedron with alternating Fe and Pt layers and terminating Pt layers, the numbers of Fe and Pt atoms is given by

$$N_{\text{Fe}} = \tfrac{1}{3}\left(5n^3 + 6n^2 + 4n\right), \quad (3a)$$

$$N_{\text{Pt}} = \tfrac{1}{3}\left(5n^3 + 9n^2 + 7n + 3\right). \quad (3b)$$

For the ordered isomers like radially ordered icosahedra and axially $L1_0$ ordered decahedra, different formation laws hold. In order to allow comparison, the excess atoms of one species have randomly been distributed over the anti-sites of the clusters, in this case. Thus, comparison of the energies and magnetic moments of different morphologies is possible since, for a given cluster size, all the different morphologies involve the same number of Fe atoms and the same number of Pt atoms as those of the perfect cuboctahedron, given by (3*a*) and (3*b*). Figure 2 shows the compositions of the investigated FePt and CoPt clusters.

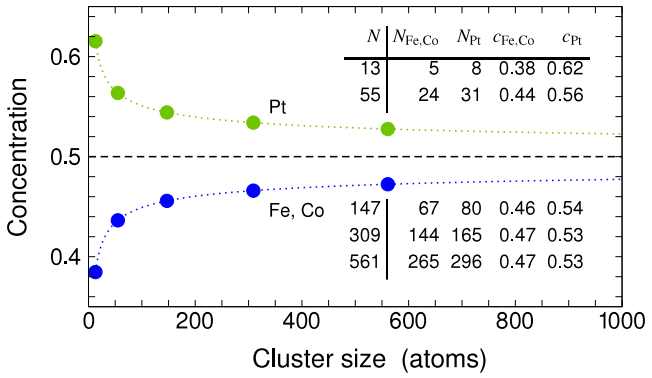

Figure 2. Compositions of the investigated FePt and CoPt clusters according to the compositions of cuboctahedra with perfect $L1_0$ order marked by the circles. Figure adapted from [15], copyright (2008) by the American Physical Society.

3. Computational results of *ab initio* cluster calculations

3.1. The FePt and CoPt clusters

Figure 3 gives an overview of *ab initio* energies of different morphologies of FePt nanoclusters (obtained with VASP) as a function of the size of the clusters with *magic* atom numbers, i.e. clusters with closed atomic shells as listed in figure 2.

As stressed before, the interest in FePt, CoPt, FePd and MnPt $L1_0$ phase nanoparticles is associated with the potential application of these materials as patterned media in magnetic recording devices. In particular, FePt with its high magnetocrystalline anisotropy, seems to be ideal for use in perpendicular recording devices. However, a close inspection of figure 3 shows that the nanoparticles with $L1_0$ structure are not lowest in energy and that other morphologies with atomic order such as icosahedra are energetically more favourable, although it is also obvious from the figure that the energy separation between the $L1_0$ structure (a) and the icosahedron with alternating Fe and Pt shells (c) is only of the order of room temperature and that this energy separation becomes smaller with increasing size of the clusters. Thus, fabrication of FePt nanoparticles in the presence of nitrogen or some other carrier gas facilitating diffusion processes during cluster growth may allow stabilization of $L1_0$ nanoclusters down to sizes of a few nanometres in diameter. However, this has not yet been achieved technically on a large lateral scale, which would make FePt nanoparticles the unique candidate for future magnetic storage devices.

The most favourable morphologies in the case of FePt nanoparticles are icosahedra with alternating arrangements of Fe and Pt shells (c), restricting Pt to every second shell starting with the surface shell. Since in icosahedra, intershell nearest-neighbour distances are a few per cent shorter than the intrashell distances, the size mismatch between Fe and Pt atoms can also be accommodated by a radial ordering of Fe-and Pt-rich layers, rather than a layer-wise $L1_0$-type alternation with tetragonal distortion, which is the case for the cuboctahedra. In icosahedra, an alternative ordering mechanism is an individual $L1_0$-type arrangement of the

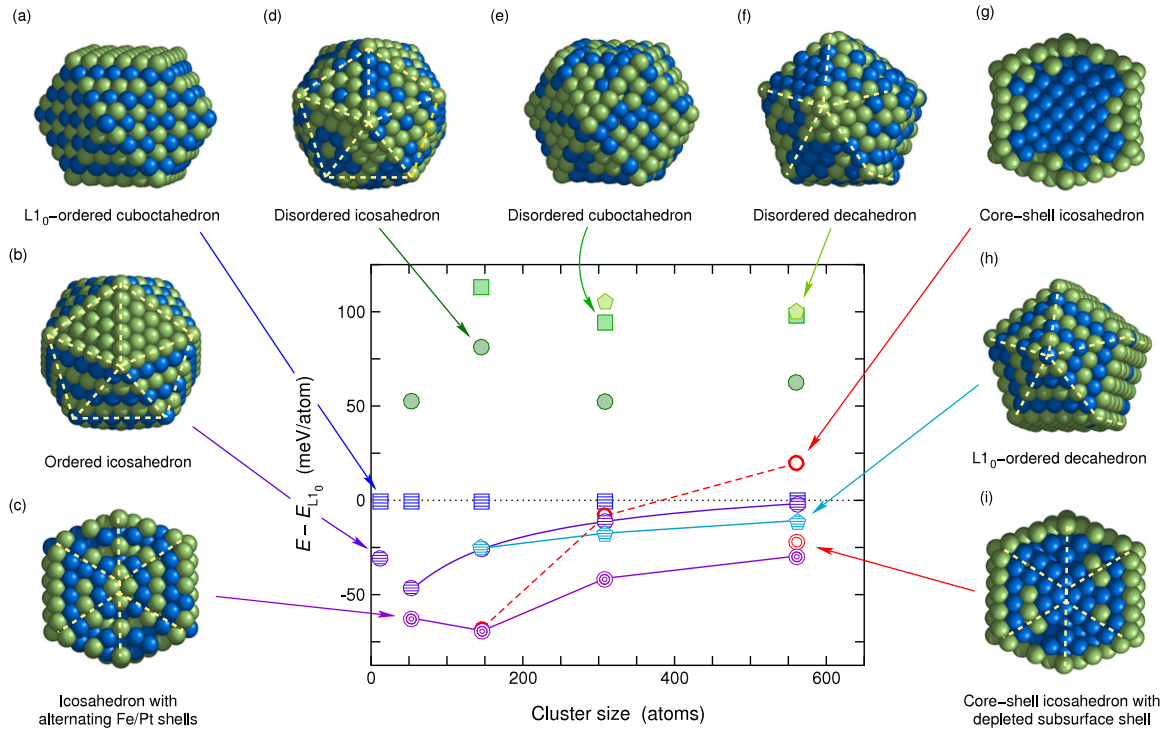

Figure 3. Energetic behaviour of different morphologies ((a)–(i)) of FePt nanoclusters as a function of the cluster size. For each cluster size, all energies are relative to the energy of the $L1_0$ cuboctahedron (a). Only structures with $N = 561$ atoms (265 Fe (dark blue) and 296 Pt (light green) atoms) are shown with arrows pointing to the symbols of the corresponding morphologies. The icosahedral structures ((c), (g) and (i)) are shown as cross sections, showing the inner arrangement of the Fe and Pt atoms. Broken yellow lines mark twin boundaries. Symbols in the diagram refer to cuboctahedra (squares), icosahedra (circles) and decahedra (pentagons); shaded green symbols denote disordered isomers, hatched blue symbols ordered structures, thick red and nested red symbols refer to corresponding core–shell icosahedra, violet triple circles to icosahedra with shellwise ordering. Figure adapted from [15], copyright (2008) by the American Physical Society.

constituents of the 20 differently oriented slightly distorted single-crystalline sections (which we call twins from now on). Such configurations have been previously discussed in terms of empirical models [20]; a related morphology is also present in our investigation as isomer (b), which was constructed by applying a full transformation along the Mackay path [21] on the position of the $L1_0$-ordered cuboctahedron (a), while retaining the original distribution of the elements on the geometric sites. The predicted crossover size in [20] is in remarkably good agreement with our study. The preference of the shellwise alternating arrangement (c) over the individual $L1_0$ ordering of the twins (b) may be related to additional stresses induced by the mismatch at the interfaces and should be expected to decrease with increasing cluster size, as the $L1_1$-type ordering (alternating Fe and Pt layers in the [111] direction) within the twins is not a particularly stable configuration for bulk FePt alloys. In contrast, fully segregated core–shell morphologies with the excess Pt atoms (that do not fit into the surface shell) randomly distributed over the sub-surface shell (g) are not a realistic model for FePt. Isomers, which are completely Pt-covered but possess an entirely Pt-depleted sub-surface shell (i), perform much better. For cluster sizes as small as those in the present investigations, morphologies (c) and (i) are closely related, since isomers (i) can be seen as a shellwise alternating arrangement with a concentration gradient in the Pt-enriched layers ranging from 0% from the centre to 100% on the surface, while in (c) the Fe and Pt concentrations remain constant for the respective shells. This close correspondence is reflected by the small energy difference; a careful optimization of the concentration gradient in the Fe and Pt layers may further improve the energy for isomer (i) w.r.t. isomer (c). In fact, icosahedral configurations with a concentration gradient have been proposed recently to explain high-resolution transmission electron micrographs of larger icosahedral FePt clusters with a diameter around 6 nm [9].

A qualitative understanding regarding the energetic tendencies of the different morphologies may be gained from comparing the density-of-states curves (DOS) of the individual morphologies. The DOS of small FePt clusters already displays basic features of bulk $L1_0$-FePt [25], but characteristic deviations exist due to the different morphologies, see figure 4. For the 561-atom FePt clusters, the differences are only partly induced by the (still important) contributions from the surface atoms, involving 45% of the atoms. The lower-energy clusters like *alternating* icosahedron (c) and $L1_0$-ordered decahedron (h) have the Fermi level coinciding with pronounced dips in the minority-spin DOS. This dip arises from the minority-spin 3d Fe electrons and is not washed out by the 3d Fe states stemming from the surface atoms (blue curves). This shows that it is mainly the 3d electrons of the transition metal element which stabilize the TM-Pt clusters. Although a similar coincidence of Fermi level and dip position exists for the $L1_0$-ordered cuboctahedron (a), it is less perfect compared to (c)

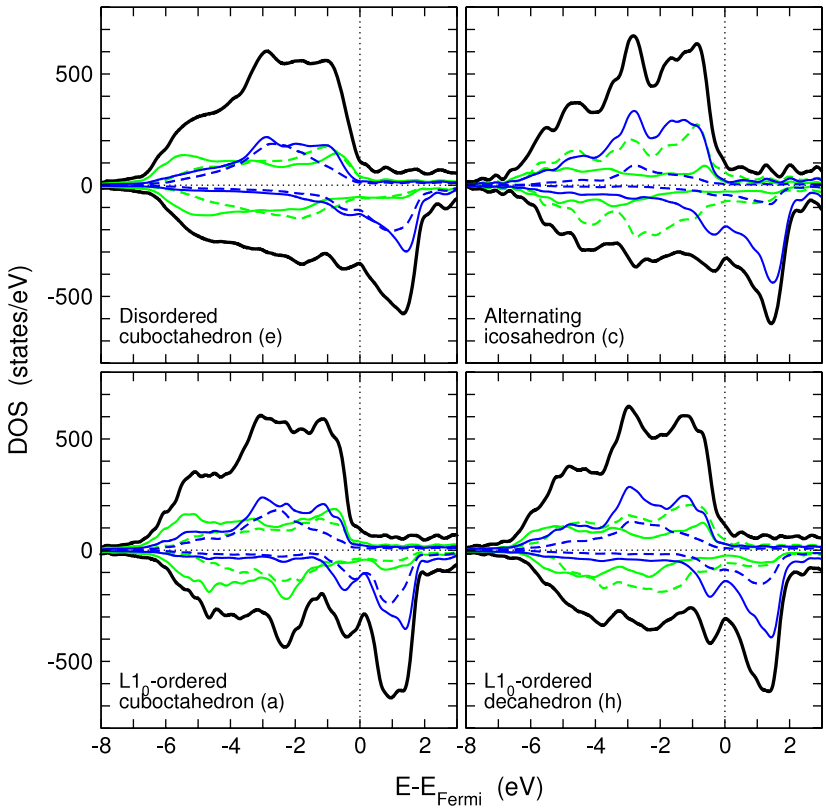

Figure 4. Variation of the spin-polarized density-of-states curves of selected $Fe_{265}Pt_{296}$-cluster morphologies: disordered cuboctahedron (e), *alternating* icosahedron (c), $L1_0$-ordered cuboctahedron (a) and $L1_0$-ordered decahedron (h), where ((e), (c), (a) and (h)) correspond to the isomers in figure 3. In each panel, the figure displays the total DOS (thick solid line), the partial DOS arising from the particle core (thin dashed lines) and the partial DOS arising from the surface atoms (thin solid lines): Fe contributions (dark blue) and Pt contributions (light green).

and (h). In the case of the disordered clusters, the dip in the minority-spin DOS is completely washed out; an inspection of figure 3 shows that the disordered clusters possess much higher energies than the $L1_0$-ordered cuboctahedron.

The magnetization of various FePt morphologies as a function of the cluster size does not show any surprising tendencies. Apart from the spin moments of morphologies (g) and (i), the magnetic moments of all the other clusters gather around 1.6 μ_B/atom [15].

Regarding CoPt nanoparticles, the situation does not really improve compared to the case of FePt nanoclusters. On the contrary, the energetic separation between ordered icosahedron, *alternating* icosahedron and core–shell icosahedron and the $L1_0$-ordered cuboctahedron is even enlarged, as is obvious from figure 5. Therefore, multiply twinned morphologies suppress large coercive fields and large magnetocrystalline anisotropy constants also in the case of CoPt nanoparticles. In addition, we observe strong segregation tendencies. Such strong segregation tendencies of Pt atoms to the surface of the clusters have recently been observed for deposited CoPt particles and have been modelled by Monte Carlo simulations [23].

However, one should underline that embedding the nanoparticles in a matrix may help to stabilize the $L1_0$ structure down to sizes of a few nm in diameter. In this context, a recent interesting attempt should be mentioned to obtain 3 nm large CoPt clusters in the $L1_0$ structure by making samples of diluted layers of CoPt clusters embedded in amorphous carbon [24].

As in the case of FePt nanoparticles, the DOS of CoPt nanoclusters tentatively allows a discussion about structural stability tendencies. To do this, we compare in figure 6 only the DOS of the $L1_0$-ordered cuboctahedron (a) and *alternating* icosahedron (c). The increased stability of the icosahedra is reflected in the DOS. Since the 3d majority-spin channel is practically *complete*, the additional d electrons of Co fill up the states in the minority-spin channel; however, there is still a difference between the DOS of (a) and (c) in that (c) displays a small stabilizing dip in the DOS around the Fermi level in both spin channels.

Regarding the behaviour of the spin moments, the same observation as for FePt can be made for CoPt nanoclusters. Isomers (g) and (h) of CoPt have somewhat reduced magnetic moments: for all other morphologies the average spin moments gather around 1.1 μ_B per atom.

3.2. The FePd and MnPt clusters

Our *ab initio* density functional theory calculations show that the formation of multiply twinned isomers with hitherto unconsidered types of chemical order are energetically favoured over the $L1_0$-ordered phase of FePt and CoPt with diameters slightly below 3 nm. The calculations for FePt clusters have meanwhile been pursued to the next *magic* number cluster, which is a 923-atom cluster. For this size, the ordered icosahedron (b) of figure 3 now has

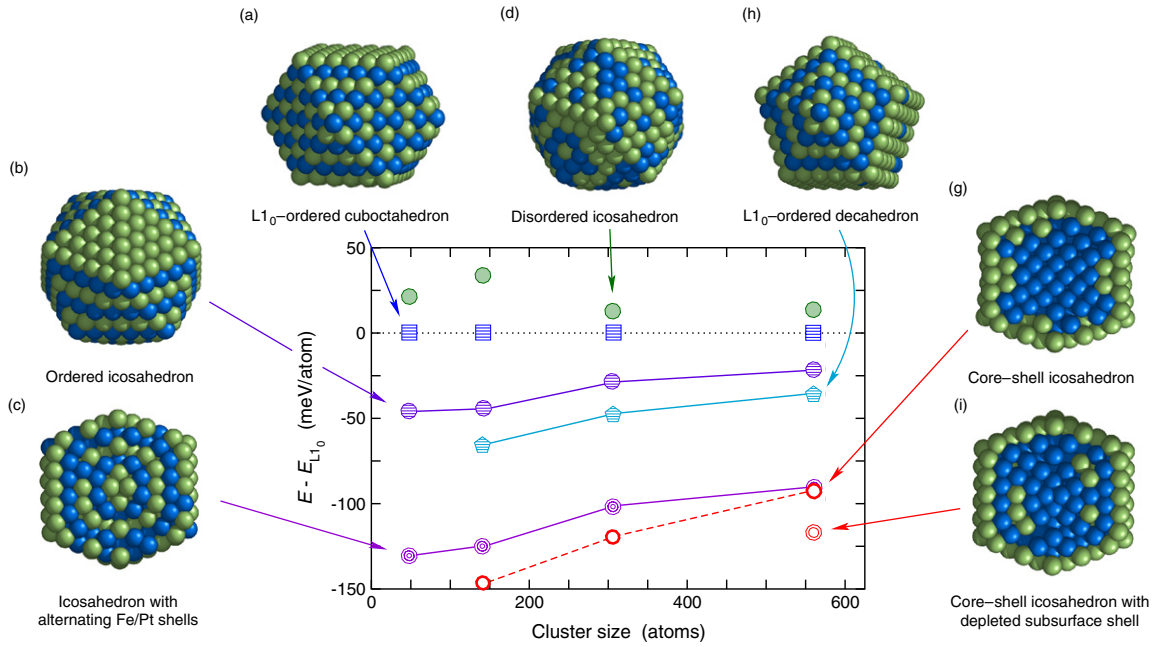

Figure 5. Energetic behaviour of different morphologies of FeCo nanoclusters as a function of the cluster size. For each cluster size, all energies are relative to the energy of the $L1_0$ cuboctahedron (a). Only structures with $N = 561$ atoms (265 Co (dark blue) and 296 Pt (light green) atoms) are shown with arrows pointing to the symbols of corresponding morphologies. The symbols defining the different morphologies are the same as used in figure 3, although the arrangement of the morphologies here differs from that in figure 3. *Alternating* and core–shell icosahedra are shown as cross sections.

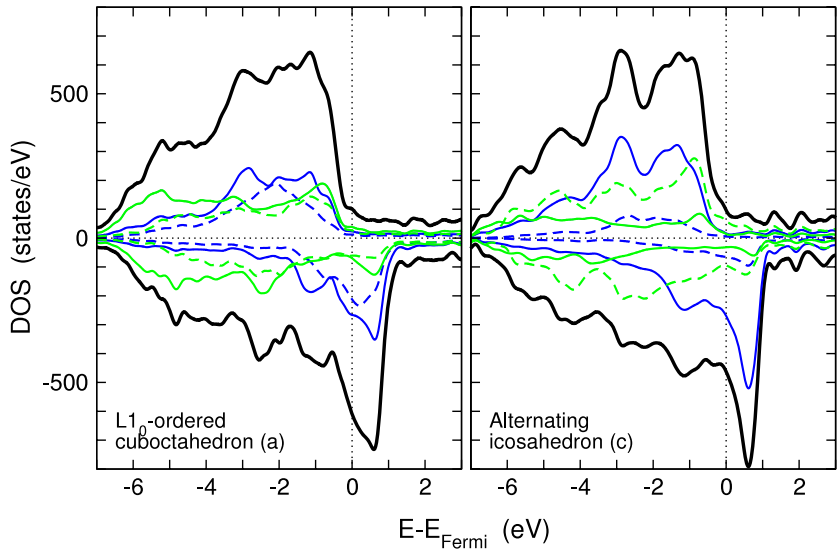

Figure 6. Variation of the spin-polarized density-of-states curves of two selected $Co_{265}Pt_{296}$-cluster morphologies: $L1_0$-ordered cuboctahedron (a) and *alternating* icosahedron (c), where (a) and (c) refer to the same isomers as in the case of FePt nanoclusters. In each panel, the figure displays the total DOS (thick solid line), the partial DOS arising from the particle core (thin dashed lines) and the partial DOS arising from the surface atoms (thin solid lines): Co contributions (dark blue) and Pt contributions (light green).

slightly higher energy than the $L1_0$-ordered cuboctahedron, indicating that there may be a critical particle size for which the technologically relevant $L1_0$ structure may become energetically most favourable compared to the energies of all other morphologies. On the basis of calculations performed, it is not sure what this critical size is for other morphologies, as, for example, isomer (c). (From an extrapolation of energy changes with cluster size in figure 3, the critical cluster size is estimated to correspond to clusters consisting of $n = 7$–9 atomic shells.) What can be confirmed so far is that, for 3 nm large FePt and CoPt particles, various multiply twinned morphologies are lowest in energy.

In order to get further insight into other transition metal clusters of that size, we have considered the case of FePd, MnPt and FeIr nanoparticles. For FePd nanoclusters with a total number of atoms up to 561, the trend for multiply twinned

structures is slightly increased compared to the FePt case [26]. MnPt clusters are particularly interesting, since they are the only clusters which we have found so far which energetically prefer the single-crystalline $L1_0$ structure. However, for magnetic storage devices, they are not really suited because of their strong antiferromagnetic order. Ternary or quaternary systems, where, for example, Mn is replaced by a sufficient amount of another 3d element (like Fe or Co) or vice versa may eventually provide the necessary crossover to ferromagnetism, which is under current investigation. FeIr clusters, on the other hand, also prefer twinned morphologies. Furthermore, layer-wise antiferromagnetism, which has been reported as a latent tendency for $L1_0$-FePt from *ab initio* calculations [19, 27, 28], is favoured over ferromagnetism for $L1_0$ morphologies for this material [29].

4. Conclusions

In this work, for each kind of binary transition metal cluster of type MnPt, FePt, CoPt, FePd and FeIr, the most probable isomers have been studied. The investigations were restricted to clusters with *magic* numbers of atoms, i.e. clusters with closed geometric shells. It is found that, for all binary clusters, apart from MnPt, the $L1_0$-ordered cuboctahedron, labelled (a) in figure 3, which is the cluster analogue of bulk layered FePt (which possesses high magnetocrystalline anisotropy, a prerequisite for use as a perpendicular magnetic recording material) is not the energetically most favoured morphology. Other morphologies of the investigated clusters, like ordered icosahedral structures, including core–shell icosahedra, are lower in energy. Thus, the theoretical investigations cannot support the use of monodisperse FePt nanoparticles down to sizes of nanoclusters with 3 nm diameter as was discussed in [1]. MnPt is special; it favours the $L1_0$ structure, but the clusters show a strong preference of antiferromagnetic order.

However, we would like to ascertain that the calculations presented here were done for free clusters. A corresponding investigation of supported clusters is under way, although we do not expect dramatic changes of the physical properties of free clusters in the case of deposited FePt clusters. The investigations of free FePt clusters point towards the possibility of a critical size of nanoparticles beyond which the ordered $L1_0$ may become energetically more favourable. For FePt clusters, this critical diameter may be around 4–6 nm, which is in agreement with the sudden increase of the coercive field of individual FePt nanoparticles observed in experiments for that size [4, 5].

Acknowledgments

The calculations were carried out on the IBM Blue Gene/L and Blue Gene/P supercomputer system of the John von Neumann Institute for Computing at Forschungszentrum Jülich. The support of the staff is gratefully acknowledged. Financial support was granted by the Deutsche Forschungsgemeinschaft within SFB 445, SPP 1239 and GRK 1240. One of us (PE) would like to thank the organizers of the International Conference on Quantum Simulators and Design, Tokyo 2008, for their invitation.

References

[1] Sun S, Murray C B, Weller D, Folks L and Moser A 2000 *Science* **287** 1989
[2] Weller D and Moser A 1999 *IEEE Trans. Magn.* **35** 4423
[3] Kubota Y, Folks L and Marinera E E 1998 *J. Appl. Phys.* **84** 6202
[4] Rellinghaus B, Stappert S, Acet M and Wassermann E F 2003 *J. Magn. Magn. Mater.* **206** 142
[5] Wiedwald U *et al* 2004 University of Ulm, unpublished
[6] Ethirajan A, Wiedwald U, Boyen H-G, Kern B, Han L, Klimmer A, Weigl F, Kästle G, Ziemann P, Fauth K, Cai J, Behm R J, Romanyuk A, Oelhafen P, Walther P, Biskupek J and Kaiser U 2007 *Adv. Mater.* **19** 406
[7] Sudfeld D, Dimitrieva O, Friedenberger N, Dumpich G, Farle M, Song C Y, Kisielowski C, Gruner M E and Entel P 2007 *Mater. Res. Soc. Symp. Proc.* **998E** 0998-J01-06
[8] Dimitrieva O, Spasova M, Antoniak C, Acet M, Dumpich G, Kästner J, Farle M, Fauth K, Wiedwald U, Boyen H-G and Ziemann P 2007 *Phys. Rev.* B **76** 064414
[9] Wang R M, Dimitrieva O, Farle M, Dumpich G, Ye H Q, Roppa H, Kilaas R and Kisielowski C 2008 *Phys. Rev. Lett.* **100** 017205
[10] Penuela J, Andreazza P, Andreazza-Vignolle C, Tolentino H C N, De Santis M and Mottet C 2008 *Phys. Rev. Lett.* **100** 11502
[11] Rossi G, Ferrando R and Mottet C 2008 *Faraday Discuss.* **138** 193
[12] Sato K, Bian B and Hirotsu Y 2002 *J. Appl. Phys.* **91** 8516
[13] Kawamura J, Sato K and Hirotsu Y 2004 *J. Appl. Phys.* **96** 3906
[14] Staunton J B, Ostanin S, Razee S S A, Gyorffy B L, Szunyogh L, Ginatempo B and Bruno E 2004 *Phys. Rev. Lett.* **93** 257204
[15] Gruner M E, Rollmann G, Entel P and Farle M 2008 *Phys. Rev. Lett.* **100** 087203
[16] Kresse G and Furthmüller J 1996 *Phys. Rev.* B **54** 11169
[17] Kresse G and Joubert D 1999 *Phys. Rev.* B **59** 1758
[18] Rollmann G, Gruner M E, Hucht A, Meyer R, Entel P and Tiago M L 2007 *Phys. Rev. Lett.* **99** 083402
[19] Gruner M E 2008 *J. Phys. D: Appl. Phys.* **41** 134015
[20] Müller M and Albe K 2007 *Acta Mater.* **55** 6617
[21] Mackay A L 1962 *Acta Crystallogr.* **15** 916
[22] Ino S 1969 *J. Phys. Soc. Japan* **27** 941
[23] Heinrichs S, Dietrich W and Maass P 2006 *Europhys. Lett.* **75** 167
[24] Tournus F, Tamion A, Blanc N, Hannour A, Bardotti L, Prével B, Ohresser P, Bonet E, Epicier T and Dupuis V 2008 *Phys. Rev.* B **77** 144411
[25] Ebert H, Bornemann S, Minár J, Dederichs P H, Zeller R and Cabria I 2006 *Comput. Mater Sci.* **35** 279
[26] Gruner M E and Dannenberg A 2008 *J. Magn. Magn. Mater.* submitted
[27] Zeng H, Sabirianov R, Mryasov O N, Yan M L, Cho K and Sellmyer D J 2002 *Phys. Rev.* B **66** 184425
[28] Brown G, Kraczek B, Janotti A, Schulthess T C, Stocks G M and Johnson D D 2003 *Phys. Rev.* B **68** 052405
[29] Gruner M E 2008 unpublished